Published in final edited form as:

J Biomed Mater Res A. 2020 January ; 108(1): 39–49. doi:10.1002/jbm.a.36790.

Bacteriophage delivering hydrogels reduce biofilm formation in vitro and infection in vivo

James A. Wroe[1,2], **Christopher T. Johnson**[1,2], **Andrés J. García**[2,3]

[1]Wallace H. Coulter Department of Biomedical Engineering, Georgia Institute of Technology and Emory University School of Medicine, Atlanta, Georgia

[2]Petit Institute for Bioengineering and Bioscience, Georgia Institute of Technology, Atlanta, Georgia

[3]Woodruff School of Mechanical Engineering, Georgia Institute of Technology, Atlanta, Georgia

Abstract

Implanted orthopedic devices become infected more frequently than any other implanted surgical device. These infections can be extremely costly and result in significant patient morbidity. Current treatment options typically involve the long term, systemic administration of a combination of antibiotics, often followed by implant removal. Here we engineered an injectable hydrogel capable of encapsulating *Pseudomonas aeruginosa* bacteriophage and delivering active phage to the site of bone infections. Bacteriophage retain their bacteriolytic activity after encapsulation and release from the hydrogel, and their rate of release from the hydrogel can be controlled by gel formulation. Bacteriophage-encapsulating hydrogels effectively kill their host bacteria in both planktonic and biofilm phenotypes in vitro without influencing the metabolic activity of human mesenchymal stromal cells. Bacteriophage-encapsulating hydrogels were used to treat murine radial segmental defects infected with *P. aeruginosa.* The hydrogels achieved a 4.7-fold reduction in live *P. aeruginosa* counts at the infection site compared to bacteriophage-free hydrogels at 7 days postimplantation. These results support the development of bacteriophage-delivering hydrogels to treat local bone infections.

Keywords

bacteriophage; biofilm; hydrogel; orthopedic; *Pseudomonas*

1 | INTRODUCTION

Implanted orthopedic devices are commonly infected surgical implants (Inzana, Schwarz, Kates, & Awad, 2016), due in part to the fact that virtually all materials used for implantable orthopedic devices are readily colonized by bacteria (Gbejuade, Lovering, & Webb, 2014; McConoughey et al., 2014), requiring 100,000-fold fewer planktonic bacteria to establish a

Correspondence: Andrés J. García, Petit Institute for Bioengineering and Bioscience, Georgia Institute of Technology, 315 Ferst Drive, Atlanta, GA 30332-0363, USA., andres.garcia@me.gatech.edu.

SUPPORTING INFORMATION

Additional supporting information may be found online in the Supporting Information section at the end of this article.

biofilm compared to living tissue (Zimmerli, Lew, & Waldvogel, 1984). Infection rates for the 1.2 million joint arthroplasties and 6 million fracture fixation procedures performed in the U.S. each year may be as high as 2 and 5%, respectively (Berríos-Torres et al., 2017; Kurtz, 2007; Yokoe, Avery, Platt, & Huang, 2013), with infection rates for compound open fractures as high as 30% (Antoci, Chen, & Parvizi, 2017; Trampuz & Zimmerli, 2006). Treatment of these infections is complicated by the formation of bacterial biofilms, which are implicated in nearly all cases of osteomyelitis (Brady, Leid, Calhoun, Costerton, & Shirtliff, 2008). Biofilms impede the ability of immune cells to reach bacteria and reduce the penetration and efficacy of antibiotics (McConoughey et al., 2014), allowing bacteria to tolerate up to 1,000 times the dose of antibiotic nominally needed to treat the same planktonic strain, and selecting for antibiotic-resistant sub-populations (Bryers, 2008; Ceri et al., 1999; Flemming & Wingender, 2010; McConoughey et al., 2014; Stewart & Costerton, 2001). Current treatments for these infections range from the use of antibiotic-doped bone cement and systemic antibiotic treatments, to surgical debridement and implant removal (Inzana et al., 2016). The antibiotic regimens needed to manage these infections systemically can have deleterious effects on the gut microbiome (Gbejuade et al., 2014; Stewart & Costerton, 2001), and current local treatments are limited by poor elution properties resulting in bacteria being exposed to sub-lethal doses, further contributing to the rise of drug-resistant strains (Erol, Altoparlak, Akcay, Celebi, & Parlak, 2004; Hagihara, Crandon, & Nicolau, 2012; Knapp, Dolfing, Ehlert, & Graham, 2010; Udou, 2004; Webb & Spencer, 2007). Furthermore, revision surgeries are associated with high rates of functional impairment, patient morbidity, and increased infection risks compared to the initial surgery (Campoccia, Montanaro, & Arciola, 2006; Gbejuade et al., 2014; Moriarty et al., 2016). All told, the complications resulting from infected orthopedic implants increase the total cost of treatment by over $50,000 per implant (Campoccia et al., 2006; Thakore et al., 2015).

These shortcomings in current treatments necessitate the development of nonantibiotic solutions to treat orthopedic device infection. One alternative is the use of bacteriophage, viruses which selectively infect and kill bacteria (Wittebole, Roock, & Opal, 2013). Bacteriophage are highly host-specific, meaning they cannot infect mammalian cells, or even other nonhost species of bacteria, avoiding unwanted effects on the patient's microbiome (Chanishvili, Chanishvili, Tediashvili, & Barrow, 2001; Chibani-Chennoufi et al., 2004; Gbejuade et al., 2014). Bacteriophage are also extremely pervasive, with nearly every known species of eubacteria having associated bacteriophage (Chanishvili et al., 2001). Furthermore, bacteriophage can propagate throughout the body in the presence of their host species, allowing single, small deliveries to produce a sustained antimicrobial effect (Sarker et al., 2012; Smith & Huggins, 1982) while remaining well tolerated by the human body (Bruttin & Brussow, 2005; Merabishvili et al., 2009; Rhoads etal., 2009; Wright, Hawkins, Änggård, & Harper, 2009). Finally, bacteriophage have evolved to be highly active against biofilm bacteria by producing enzymes and other factors that degrade the biofilm matrix (Cornelissen et al., 2011; Harper et al., 2014; Phee et al., 2013). Recent research has explored their use as coatings for urinary and intravenous catheters to prevent biofilm formation (Curtin & Donlan, 2006; Fu etal., 2009; Lehman & Donlan, 2014). Clinical studies have investigated applying solutions of bacteriophage to infection sites as an alternative to traditional antibiotic therapies (Merabishvili et al., 2009; Rhoads et al., 2009;

Wright et al., 2009). While promising, these treatment strategies are limited by the sudden release of the bacteriophage into a microenvironment from which they will rapidly disperse and be eliminated without sufficient concentrations of their host bacteria (Lehman & Donlan, 2014). Therefore, more controlled methods of delivering bacteriophage to implant sites are required.

We previously developed a hydrogel synthesized from the reaction of maleimide groups in a four-arm poly(ethylene glycol)-4-maleimide (PEG-4MAL) macromer with the free thiols in a di-thiolated crosslinker, typically a protease-degradable, cysteine-containing peptide (García, Clark, & García, 2016; Phelps et al., 2011). This hydrogel can be functionalized with thiolated molecules such as cell adhesion peptides and can be engineered to deliver peptides, proteins, or even cells by encapsulating them in the gel so they can be released by diffusion or by degradation of the gel (Phelps et al., 2011). The rapid polymerization of this hydrogel allows for in situ delivery with adherence to exposed surfaces while restricting delivery of its payload only to the local micro-environment, and its customizable chemistry means release of its payload can be tuned to the relevant microenvironment (García et al., 2016). We previously demonstrated the potential of this scaffold in osseoregenerative applications by showing first that it improves bone repair when used to deliver bone morphogenetic protein 2 (BMP-2) compared to BMP-2-soaked collagen sponges (Shekaran et al., 2014), and demonstrating that hydrogel-mediated lysostaphin delivery eliminates methicillin-resistant *S. aureus* (MRSA) infection in bone fractures (Johnson et al., 2018). While staphylococcal infections account for 66% of orthopedic hospital-acquired infections (HAIs; Campoccia et al., 2006), the use of lysostaphin is not easily generalizable to other genera of bacteria (Johnson et al., 2018; Schindler & Schuhardt, 1964). As such, continued development of treatment strategies for other bacterial species implicated in orthopedic infections is still required.

In this study, we engineered hydrogels for controlled delivery of bacteriophage targeting *Pseudomonas aeruginosa* to the site of orthopedic infections (Figure 1). *P. aeruginosa* accounts for 8% of all HAIs (Campoccia et al., 2006; McConoughey et al., 2014) and 13% of multidrug-resistant HAIs (Hidron et al., 2008), making it the most common Gram-negative bacteria implicated in orthopedic implant infections (Brouqui, Rousseau, Stein, Drancourt, & Raoult, 1995; Campoccia et al., 2006; McConoughey et al., 2014). Clinical isolates of *P. aeruginosa* have particularly high rates of single and multi-antibiotic resistance (Hidron et al., 2008; Hirsch & Tam, 2010), and an elevated tendency to develop resistance during treatment due to the species' ability to dynamically regulate encoded resistance mechanisms (Lister, Wolter, & Hanson, 2009; Paramythiotou et al., 2004). Consequently, osteomyelitis involving *P. aeruginosa* has 2.5 times the recurrence rate of *S. aureus* osteomyelitis and an increased risk of amputation compared to other species (Tice, 2003), making the strain of particular clinical relevance.

We characterized the release of bacteriophage from different protease-degradable hydrogels. We then designed a platform to grow biofilms on surfaces in vitro and evaluated the antibiofilm properties of the phage-encapsulating hydrogel. Finally, we evaluated the ability of bacteriophage-delivering hydrogels to reduce *P. aeruginosa* infection in a murine radial

segmental defect model and tested whether the bacteriophage-encapsulating gel was tolerated in vivo.

2 | MATERIALS AND METHODS

2.1 | Selection and culture of bacterial strains

The bacterial strains used in the study have been described previously (Fu et al., 2009). PsAer-9 was selected for its biofilm formation ability and because of its broad susceptibility to a range of *P. aeruginosa* bacteriophage from a collection of *P. aeruginosa* strains from the Clinical and Environmental Microbiology Branch at the CDC (Lehman & Donlan, 2014). This strain was then modified to express luciferase when growing in biofilm through a triparental mating scheme (Escapa, Cerro, García, & Prieto, 2012). *Escherichia coli* MG1655 containing the pSEVAplaxA plasmid (kanamycin resistance, ori RSF1010 replicon, PlexA driving luxCDABE) was used as the donor strain, *E. coli* pKR6OO was used as the helper strain, and PsAer-9 was the recipient (Silva-Rocha et al., 2012).

Liquid cultures of this modified PsAer-9 were prepared by spotting frozen bacteria isolates on trypticase soy agar (TSA) (BD Diagnostics) containing 50 μg/ml kanamycin (ThermoFisher Scientific, Waltham, MA) and incubating at 37°C for 24 hr, then incubating single colonies from the plate at 37°C overnight in 5 ml of 25% trypticase soy broth (TSB; BD Diagnostics, Franklin Lakes, NJ) containing 50 μg/ml kanamycin with shaking at 200 rpm.

2.2 | Culture and quantification of bacteriophage

Isolation of the *P. aeruginosa* bacteriophage strains used in this study has been described previously (Fu et al., 2009). ΦPaer4, ΦPaer14, ΦPaer22, ΦW2005A (P *aeruginosa),* and ΦK (S. *aureus;* American Type Culture Collection) were selected for this study because of their broad infectiousness across several strains of their host bacteria (Fu et al., 2009). Phages were propagated by adding samples to liquid cultures of 25% TSB containing 10^7-10^8 CFU/ml of their host bacteria and incubated at 37°C until bacterial lysis was observed. 2% v/v chloroform (Sigma-Aldrich, St. Louis, MO) was added to the solution, which was then centrifuged, and the supernatant was filtered through a 0.2 μm pore membrane. These bacteriophage cultures were further concentrated and purified by anion-exchange chromatography (Agarwal et al., 2018). Endotoxin was removed using EndoTrap Red (Hyglos) column per the manufacturer's instructions.

Bacteriophage quantification plates were created by combining 100 μl samples of a liquid culture of the host bacteria with optical density (OD) of 0.5 (approximately 5×10^8 colony-forming units per ml [CFU/ml]; MicroScan Turbidity Meter; Siemens, Washington, DC), with 3 ml of soft agar, pouring this mixture over TSA, and allowing it to set. Concentration of live bacteriophage in liquid samples was calculated by plating 10 μl of 10x serial dilutions of the original sample in PBS (Mediatech) on these plates, incubating the plates at 37°C for 24 hr, and enumerating visible plaques in the most concentrated dilution of each sample with no overlapping plaques.

2.3 | Bacteriophage host specificity assay

Samples (25 μl) of PBS, or 2×10^9 PFU/ml ΦPaer4, ΦPaer14, or ΦK stocks were introduced to 5 ml liquid cultures of PsAer-9 containing 5.6×10^7 CFU/ml. OD of the samples at 590 nm was measured every 30 min for 6 hr.

2.4 | Bacteriophage-encapsulating hydrogels

An adhesive peptide, either GRDGSPC (RGD) or GGYGGGPC$(GPP)_5$ GFOGER$(GPP)_5$GPC (GFOGER) (AAPPTec), and one of the crosslinkers GCRDVPMSMRGGDRCG (VPM), GCRDGPQGIWGQDRCG (GPQ-W) (Genscript), or dithiothreitol (DTT; Sigma-Aldrich) were both combined in 100 mM MES buffer (Sigma-Aldrich), pH 6.0–6.5. This solution was then combined with PBS for sterile gels, a stock of purified bacteriophage for bacteriophage-encapsulating gels, PsAer-9 inoculum for infected gels, or PsAer-9 inoculum mixed with a bacteriophage stock for infected bacteriophage-encapsulating gels. For in vitro studies, this mixture was combined on Parafilm or inside a PDMS (Dow Corning, Midland, MI) microfluidic device with 20 kDa PEG-4MAL macromer (Laysan Bio, Arab, AL) in 100 mM MES buffer, pH 6.0–6.5 and allowed to polymerize for 15 min at 37°C in a humidified, 5.0% CO_2 incubator. For in vivo studies, 3 μl of the relevant hydrogel was polymerized and loaded into a 4.0 mm perforated polyimide sleeve. These implants were then fit over a murine radial defect, such that the hydrogel filled the defect space.

Final concentrations of the components in the hydrogels were 4.0% wt/vol PEG-4MAL (20-kDa), and 1.0 mM adhesive peptide, with the amount of crosslinker stoichiometrically proportional to the number of remaining maleimide groups after accounting for incorporation of the adhesive peptide. Unless specified otherwise, the crosslinker used to polymerize these hydrogels was VPM. All hydrogels used in in vitro experiments used RGD as the adhesive peptide. We used GFOGER instead of RGD for the in vivo experiments because GFOGER-functionalized gels produce superior bone healing compared to RGD-functionalized hydrogels (Shekaran et al., 2014). Hydrogels used in in vivo studies further contained 30 ng of BMP-2 (R&D Systems, Minneapolis, MN) per gel, as we previously showed that this BMP-2 dose delivered from this hydrogel system produced extensive bone repair without inducing potentially pathophysiological over-growth compared to lower and higher doses delivered to the murine radial defect model. We have previously demonstrated no differences in mechanical properties or protein release between RGD-and GFOGER-presenting hydrogels (García et al., 2016). The specific concentrations and strains of bacteria and bacteriophage used in each experiment are specified in the relevant methods section.

2.5 | Bacteriophage release from hydrogels in vitro

Hydrogels (25 μl) crosslinked with either VPM or GPQ-W containing 5.6×10^7 PFU of ΦPaer14 per gel were submerged in 1.0 ml of either PBS with calcium and magnesium or 0.5 U/ml collagenase II in PBS with calcium and magnesium in a 24 well plate and maintained at 37°C. About 10 μl of the supernatant was sampled from the wells at 8, 17, 31, or 105 hr and plated on PsAer-9 to calculate the number of released bacteriophage.

The effects of the rate of release of bacteriophage on the growth of PsAer-9 in liquid solution was assessed by placing 25 μl hydrogels encapsulating 8.0×10^6 PFU/gel each of ΦPaer4, ΦPaer14, ΦPaer22, and ΦW2005A into screw cap culture tubes containing 5 ml of 25% TSB inoculated with 5.6×10^7 CFU/ml CFU PsAer-9. Collagenase (40 U/ml) was added to specified samples. Gels were crosslinked with either VPM, GPQ-W, or nonproteolytically degradable DTT. Culture tubes were then incubated at 37°C and shaken at 200 rpm. OD of the culture tubes at 590 nm was measured every 30 min for 6 hr.

2.6 | In vitro biofilm growth

Acrylic chips containing an 18 mm × 1.5 mm × 1.5 mm (40 μl) central channel were attached to glass microscope slides with UV-activated glue. Hydrogels (25 μl) were polymerized in the channel. Bacteriophage-delivering hydrogels contained 1.0×10^7 PFU/gel, while control gels were made by substituting the bacteriophage stock with an equal volume of pH 6.0–6.5 100 mM MES. A microfluidic device was then placed over the channel and attached with UV activated glue by 1-min exposure to 300 nm light. The device was then placed on a hot plate set to 37°C. A liquid culture of PsAer-9 was diluted to an OD of 0.5 at 590 nm, and drawn through the microfluidic device over the surface of the gel by a syringe pump at 5 μl/min for 1 hr, followed by 24 hr of 25% TSB containing 50 μg/ml kanamycin drawn through the system at the same rate. Based on the estimated hydraulic diameter of the flow channel (1.15 mm), fluid velocity (3.6 mm/min, and kinematic viscosity of water (7×10^{-3} cm^2/s), we calculate a Reynolds number of 9.7×10^{-6}, so the flow through the device was assumed to be laminar.

To test whether UV light exposure or another step in the device manufacturing process affect ΦPaer14 viability, ΦPaer14-encapsulating hydrogels (25 μl) containing 1.0×10^7 PFU/gel were placed in a UV-curing oven for 2 min (the total amount of time the gels are exposed to UV light during the microfluidic device assembly process), then degraded in 100 μl of 385 U/ml collagenase II in a 37°C water bath for 1 hr. This liquid sample was diluted with 900 μl of PBS and plated on PsAer-9 to determine the concentration of live bacteriophage remaining in the gel.

2.7 | In vitro activity of bacteriophage against biofilms

The effects of bacteriophage on the growth and adherence of bacteria on the surface of hydrogels was assessed by weighing each hydrogel, then degrading it for 1 hr in 100 μl of 385 U/ml collagenase II in a 37°C water bath. This sample was diluted with 900 μl PBS, and 10 μl serial dilutions of this sample were plated on TSA and incubated overnight. Colonies in the highest concentration sample that produced distinct colonies were counted to derive the concentration of bacteria present on the original gel sample.

After biofilm formation, bacteria were stained with fluorescent dyes by flowing them over the biofilms at 5 μl/min for 20 min. Black and white images of the samples were acquired on a Nikon TE300 inverted microscope using a Plan Fluor 20X objective (Nikon) and subsequently pseudocolored in Photoshop CS6 (Adobe). The live/dead dye used was a 10 μl 1:1 mixture of 3.34 mM SYTO 9 in DMSO and 20 mM propidium iodide in DMSO (ThermoFisher, Waltham, MA) diluted in 990 μl of PBS. Live and dead images were taken

at 485 and 535 nm respectively. FilmTracer SYPRO Ruby biofilm stain (ThermoFisher) was used for biofilm staining and images were taken at 535 nm.

2.8 | Human mesenchymal stromal cell cytocompatibility

Human mesenchymal stromal cells (hMSCs) obtained from the NIH Resource Center at Texas A&M University were plated in a 96 well plate (5,000 cells/well) and incubated in 200 μl of hMSC media for 24 hr. Media were then replaced with either 200 μl of unaltered hMSC media or hMSC media containing 2×10^6 PFU/μl, and cultured for an additional 24, 48, or 72 hr. Cell metabolic activity was then assessed by incubating the cells with a 10% solution of CCK-8 reagent (Dojindo) for 45 min and measuring fluorescence intensity at 450 nm.

2.9 | Murine radial segmental defect model

All animal experiments were conducted under protocols approved by the Georgia Tech Animal Care and Use Committee. Experiments were performed on 8–10 weeks old male C57/B6 mice, housed in 12 hr light/dark cycles and given free access to food and water. Mice were anesthetized with 1.5% isoflurane inhalation and their right hindlimb was injected with 1 mg/kg buprenorphine as an analgesic. A 1 cm incision was made over the radius, and a bone cutting tool was used to remove 2.5 mm of the radius. About 3 μl hydrogels loaded in 4.0 mm perforated polyimide sleeves were fitted over the ends of the radius spanning the defect. The wound was then sutured shut. Bacteria-encapsulating gels contained 3.0×10^4 CFU of PsAer-9. Bacteria/bacteriophage-encapsulating gels contained 3.0×10^4 CFU of PsAer-9 and 1.2×10^8 PFU/ml each of ΦPaer4, ΦPaer14, ΦPaer22, and ΦW2005A. All hydrogels used in vivo contained 30 ng of BMP-2 per implant.

2.10 | Quantification of bacteria and bacteriophage in tissue

Mice with either bacteria or bacteria/bacteriophage encapsulating-hydrogels were euthanized via CO_2 inhalation at 1 week. After euthanasia implants were dissected from the mouse with surrounding tissue, isolated, then pulverized by mortar and pestle. Single bacterial cell suspensions were then created with a series of sonicating and vortexing steps (sonicate 10 min, vortex 30 s, sonicate 5 min, vortex 30 s, sonicate 30 s, vortex 30 s). Serial dilutions of these liquid suspensions were plated on TSA to enumerate bacteria and on PsAer-9 to enumerate bacteriophage.

2.11 | Histology

Following euthanasia, the radius and surrounding tissue were removed and fixed in 10% neutral buffered formalin (Sigma-Aldrich), then decalcified in formic acid (Sigma-Aldrich), embedded in paraffin, and prepared into 5 μm sections. Samples were deparaffinized, rehydrated, and stained using hematoxylin and eosin, and imaged with a Nikon Eclipse E600 microscope using a Plan Fluor 20× objective (Nikon), Micropublisher 5.0 RTV (Q imaging) color camera, and Q-Capture software (Q imaging).

2.12 | Mechanical testing of hydrogels

Mechanical testing of hydrogels was performed using a Modular Compact Rheometer 302 (Anton Paar, Graz, Austria) with a CP10–2 measuring cone (Anton Paar) with data measured and recorded in RheoCompass. About 25 μl control and bacteriophage-encapsulating hydrogels were polymerized on parafilm, then placed on the rheometer along with 10 μl of PBS to avoid sample dehydration. Storage modulus (G') and loss modulus (G'') were calculated from the linear regions of their respective stress-strain curves as found by amplitude sweeps performed according to the manufacturer's instructions.

2.13 | Statistics

Single test groups were compared to controls using an unpaired Student's *t* test, unless samples had significantly different variances (in which case Welch's t test was used), or had non-normal distribution (in which case a Mann-Whitney *U* test was used). Experiments comparing multiple groups were performed using ANOVA comparing all test groups, followed by Tukey's test for multiple comparisons. Outliers were detected using a ROUT test with a false discovery rate of 1%. Values of PFU or CFU per unit volume were transformed by $\log_{10}$ before analysis. All analyses were performed using Prism Graphpad 7.

3 | RESULTS

3.1 | Bacteriophage encapsulated in PEG-4MAL hydrogels retain bactericidal activity

To confirm that the *P. aeruginosa* strain PsAer-9 used in this study was sensitive to *P. aeruginosa* bacteriophage, we prepared low titre liquid cultures of PsAer-9 and exposed them to PBS, *P. aeruginosa* bacteriophage ΦPaer4 or ΦPaer14, or S. *aureus* bacteriophage ΦK, and monitored the OD of these solutions over 6 hr (Figure 2). Cultures treated with *S. aureus* bacteriophage or no bacteriophage showed a 14.5-fold and 9.7-fold increase in OD respectively and no significant difference in OD, whereas cultures treated with *P. aeruginosa* bacteriophage had no significant change in OD over the 6 hr treatment time and showed a significantly lower OD at 6 hr compared to the untreated and S. *aureus* bacteriophage-treated groups. There were no differences between groups treated with a single *P. aeruginosa* bacteriophage or a combination of *P. aeruginosa* bacteriophage.

We hypothesized that release of bacteriophage encapsulated in hydrogel could be controlled by degradation of the hydrogel by proteases present in vivo. To determine whether the PEG-4MAL platform could be used to deliver encapsulated bacteriophage and modulate the rate of bacteriophage release into the environment, we formulated PEG-4MAL gels containing the RGD adhesive peptide polymerized with one of the protease-degradable crosslinkers, VPM or GPQ-W, in the presence of live ΦPaer14. These two crosslinking peptides have different proteolytic rates (Patterson & Hubbell, 2010). We placed these bacteriophage-encapsulating hydrogels in either PBS or a PBS solution containing collagenase, and sampled the supernatant periodically over 105 hr to monitor concentration of released bacteriophage (Figure 3). VPM-crosslinked gels in the presence of collagenase had the highest rate of phage release, achieving 50% release by 8 hr, sevenfold faster than GPQ-W crosslinked gels in collagenase, which had the next highest release rate. VPM-crosslinked gels in collagenase were also the only test condition to completely release their

payload of encapsulated bacteriophage within the tested time period, which they did by 17 hr. At this same time point, GPQ-W crosslinked gels exposed to collagenase had released 8% of their payload, while VPM-and GPQ-W crosslinked gels incubated in PBS without collagenase had released 0.16% and 0.04% of their respective payloads.

To determine the effect of crosslinker selection on the growth of populations of live bacteria, hydrogels encapsulating a combination of bacteriophage (ΦPaer4, ΦPaer14, ΦPaer22, and ΦW2005A) were synthesized as above with either VPM, GPQ-W, or nonproteolytically degradable DTT as the crosslinker. These gels were placed in liquid cultures of *P. aeruginosa* with collagenase and an additional control group of VPM-crosslinked gels was placed in a *P. aerugniosa* culture without collagenase. OD at 590 nm of these cultures was monitored over 6 hr and compared to the change in OD of *P. aeruginosa* cultured over the same time period in the presence of a bacteriophage-free hydrogel (Figure 4). The VPM and GPQ-W groups in collagenase showed significantly lower OD at 6 hr compared to the normal growth curve of the untreated group. Gels polymerized with the VPM crosslinker produced the lowest final OD of all samples tested. Samples crosslinked with DTT and samples tested in the absence of collagenase showed no difference from the standard growth curve. This results further illustrates that control over the cross-linking peptide modulates the antimicrobial efficacy of the hydrogel, with faster degrading peptide sequences leading to faster elimination of the pathogen by release of active bacteriophage.

3.2 | Hydrogel-encapsulated bacteriophage reduce the formation of biofilms

Biofilms form when bacteria attach to a surface and surround themselves with an insoluble polymer matrix, providing the bacteria with increased resistance to the host immune system and antibiotics (Bryers, 2008; Flemming & Wingender, 2010; McConoughey et al., 2014; Stewart & Costerton, 2001). Pilot studies showed poor development of biofilms on hydrogels under static conditions, likely due to the inherent nonfouling properties of the gel. Because biofilm formation for *P. aeruginosa* is enhanced when shear flow-sensing extracellular polysaccharides indicate to the bacterium that it has adhered to a surface (Kievit, 2009; Rodesney et al., 2017), we designed a laminar flow microfluidic device to produce consistent fluid shear over a surface to promote bacteria adhesion and biofilm development (Figure 5a,b). Untreated hydrogels were cast in acrylic troughs designed to hold test material under the flow channel of microfluidic device, and liquid cultures of PsAer-9 were allowed to adhere to and grow on the surface of the hydrogel under static or constant flow conditions for 24 hr. Fluorescence staining of live bacteria and biofilm-associated proteins revealed more live adherent bacteria and biofilm-associated proteins in the hydrogels cultured under constant flow conditions, indicating an established biofilm microenvironment (Figure 5c–f).

After confirming that ΦPaer14 remained viable through both the assembly of the microfluidic device (Figure S1) and the biofilm generation protocol (Figure 6a), we tested whether hydrogel-encapsulated ΦPaer14 maintained antimicrobial activity against *P. aeruginosa* biofilms by culturing PsAer-9 over untreated and phage-encapsulating hydrogels under constant flow conditions for 24 hr. Significantly fewer live bacteria were recovered from bacteriophage-encapsulating gels compared to control gels, with 17-fold fewer CFUs

counted per mg of recovered hydrogel and 16.9-fold fewer CFUs counted per whole hydrogel (Figure 6b,c). Analysis of fluorescence staining showed higher levels of live bacteria and biofilm-associated proteins on control gels compared to phage-encapsulating gels and higher levels of dead bacteria on ΦPaer14-encapsulating hydrogels compared to control gels (Figure 6d–i). Bacteriophage plaques were also observed on ΦPaer14-encapsulating hydrogels stained for live bacteria and biofilm matrix proteins (Figure 6e,i).

3.3 | Bacteriophage-containing hydrogels reduce bacterial infection in bone defects

We first confirmed the in vitro cytocompatibility of ΦPaer14 with hMSCs by placing ΦPaer14-encapsulating hydrogels in the culture media of hMSCs and assessing hMSC metabolic activity at 24, 48, and 72 hr. We observed no significant differences in metabolic activity between hMSCs cultured in the presence of these gels compared to controls at 24 and 48 hr, and a small (13%) but significant increase in the metabolic activity in the hydrogel group compared to the control at 72 hr (Figure 7a). Next, to test whether bacteriophage is well tolerated at bone defect sites in vivo, we polymerized BMP-2 laden ΦPaer14-encapsulating hydrogels within a perforated polyimide sleeve and fitted this sleeve over the site of a segmental defect in the murine radius (no infection) such that the hydrogel filled the defect space, and recovered the hydrogels and surrounding tissue at 1 or 4 weeks (Figure 8). Histology of these samples showed no gross differences for tissue surrounding the implant between sterile and ΦPaer14-encapsulating gels at either time point, indicating equivalent inflammatory responses.

We next tested the ability of bacteriophage-encapsulating hydrogels functionalized with GFOGER and BMP-2 to reduce infection in vivo. Rheological analyses demonstrated no differences in mechanical properties between bacteriophage-encapsulating and control hydrogels (Figure S2). We placed hydrogels containing live *P. aeruginosa* and a bacteriophage mixture at radial segmental defects in mice and recovering the hydrogels and surrounding tissue at 1 week to quantify the number of live bacteria and bacteriophage (Figure 9a,b). Gels containing a combination of *P. aeruginosa* bacteriophage (ΦPaer4, ΦPaer14, ΦPaer22, and ΦW2005A) were used in this experiment to reduce the risk of bacteria developing tolerance to the phage. *P. aeruginosa* was co-delivered with the bacteriophage in infection models to ensure consistent initial exposure conditions between the different test animals. Defects treated with control hydrogels showed high numbers of live bacteria, indicating the presence of an established infection. Defects treated with bacteriophage-encapsulating gels contained 4.7-fold fewer live bacteria compared to controls, approximately 7.4×10^3 CFU per implant (Figure 9a). Furthermore, bacteriophage were only recovered from the bacteriophage-delivering hydrogel (Figure 9b), demonstrating active phage infection of the host bacteria.

4 | DISCUSSION

Bone fractures and nonunion defects often require surgical intervention where biomedical devices are used to correct the defect, but 5–10% of these procedures are compromised by bacterial infection. Current clinical treatment options are limited to sustained, high doses of antibiotics and surgical debridement of affected tissue. These corrective procedures

significantly drive up healthcare costs and have sub-optimal patient outcomes as effective antibiotic doses are difficult to attain at the site of the infection due to the presence of a biofilm and toxicity considerations. Furthermore, the emergence of antibiotic-resistant bacteria raises concerns regarding the effectiveness of current antibiotics to reduce biomaterial-associated infections. Therefore, there is a significant, unmet need for alternative therapeutic strategies to eliminate device-related infections.

Biomaterial platforms to deliver antimicrobial agents, such as antibiotics and antimicrobial peptides, or present polymers with bactericidal properties have emerged as powerful technologies to combat infection (Caplin & García, 2019). For example, we recently reported on synthetic hydrogels with controlled delivery of the antimicrobial enzyme lysostaphin that eliminate bone infections and promote the repair of bone fractures and nonhealing segmental bone defects (Johnson et al., 2018; Johnson et al., 2019). Although very promising, this strategy is limited to Gram-positive staphylococcal species. In the present study, we engineered synthetic hydrogels to deliver bacteriophage against *P. aeruginosa,* an important Gram-negative pathogen. Bacteriophage retain their bacteriolytic activity after encapsulation and release from the hydrogel, and their rate of release from the hydrogel can be controlled by gel degradation. Bacteriophage-encapsulating hydrogels effectively kill their host bacteria in both planktonic and biofilm phenotypes in vitro without influencing the metabolic activity of hMSCs. Finally, bacteriophage-encapsulating hydrogels significantly reduced bacteria counts in a murine segmental bone defect at 7 days postimplantation. These results provide initial steps in the development of bacteriophage-delivering hydrogels to treat local bone infections. A limitation of our study is that the bacteria and bacteriophage were co-delivered at the time of implantation. Whereas this approach only mimics a prophylactic infection scenario, it provides a reproducible infection model comprising one surgical procedure. Future studies should consider therapeutic scenarios where an infection is first established and then treated. In addition, we examined bacteria counts at 7 days posttransplantation but did not explore whether the hydrogels promote bone repair at longer time points. The ability of bacteriophage-delivering hydrogels to heal these bone defects will be the subject of future studies. We note our recent study demonstrating that lysostaphin/BMP-2-delivering hydrogels eliminated *S. aureus* infection and supported full bone defect repair at 8 weeks in the same murine segmental model (Agarwal et al., 2018; Johnson et al., 2019).

Bacteriophage have been explored as therapeutic agents for decades but have received renewed interest with recent clinical cases (Dedrick et al., 2019; Jennes et al., 2017; Schooley et al., 2017). Most common strains of bacteria implicated in orthopedic implant-associated infections have identified bacteriophage (Campoccia et al., 2006; Wittebole et al., 2013), making the approach used to prevent *P. aeruginosa* colonization in this study generalizable to a broad spectrum of organisms involved in clinical bone infections and osteomyelitis. Indeed, recent research has explored the use of bacteriophage to treat bone infections (Kaur, Harjai, & Chhibber, 2014, 2016; Kishor et al., 2016; Meurice et al., 2012; Nir-Paz et al., 2019; Yilmaz et al., 2013). Future studies could investigate the delivery of multiple bacteriophage targeting different genera such a *Staphylococcus* and *Enterococcus,* and explore their ability to combat the complex, multispecies biofilms often found in clinical osteomyelitis cases (Bryers, 2008). This, combined with previous work demonstrating the

viability of this hydrogel platform as a scaffold for bone repair, make bacteriophage-encapsulating PEG-4MAL hydrogels a viable prospect for use as a prophylactic in orthopedic surgeries and as a treatment option for revision surgeries involving established infections. Our results show that the rate of release of bacteriophage from the hydrogel can be tuned as a function of gel composition supports this range of applications where different release profiles might be desirable.

The dependence of bacteriophage on specific surface proteins to adhere to and infect their hosts means that it is possible that bacteria could eventually evolve resistance to bacteriophage therapies in the same way that they have to small molecule antibiotics (Chanishvili et al., 2001; Yilmaz et al., 2013), although the ability of bacteriophage to co-evolve with their hosts may limit this effect (Lenski & Levin, 1985; Sweere et al., 2019). Notably, Yilmaz et al. found that co-delivery of bacteriophage and antibiotics had a synergistic effect on reducing both methicillin-resistant *Staphylococcus aureus* (MRSA) and *P. aeruginosa* infections, including in biofilms, providing a much greater reduction in viable bacteria compared to either treatment used individually (Yilmaz et al., 2013). The versatility of the hydrogel scaffold used in this study makes exploring co-delivery of bacteriophage and antibiotics through this platform a viable option, with the added benefit that the localized delivery provided by the platform means higher concentrations of antibiotic than would normally be considered safe for systemic delivery could be used, reducing the risk of delivering sub-lethal doses to a biofilm. In addition to the development of resistance, recent evidence revealed that bacteriophage strains can trigger antiviral immunity and prevent clearance of bacteria (Mizoguchi et al., 2003), so it will be critical to screen and select phage strains that infect and kill target bacteria.

5 | CONCLUSION

We engineered an injectable hydrogel capable of encapsulating active bacteriophage and delivering them to the site of bone infections. The scaffold was able to deliver live bacteriophage after encapsulation, and significantly reduced the number of live *P. aeruginosa* bacteria in both planktonic and biofilm phenotypes in vitro. Importantly, this bacteriophage-encapsulating hydrogel significantly reduced *P. aeruginosa* infection in a murine radial defect model while showing similar gross host responses to bacteriophage-free hydrogels. This study supports further investigation of this material for the prevention of orthopedic implant infections.

Supplementary Material

Refer to Web version on PubMed Central for supplementary material.

ACKNOWLEDGMENTS

The pSEVAplexA plasmid was kindly provided by Victor de Lorenzo. The *Pseudomonas* bacteriophage used in this study was kindly provided by Rodney Donlan. Transfection of the pSEVAplexA plasmid into PsAer-9 was performed by Nina Dinjaski and Auxiliadora Prieto. We thank the core facilities at the Parker H. Petit Institute for Bioengineering and Bioscience at the Georgia Institute of Technology for the use of their shared equipment, services and expertise. Research reported in this publication was supported by the National Institute of Arthritis and Musculoskeletal and Skin Diseases of the National Institutes of Health under Award Number R01AR062920 (A.J.G.) and F30AR069472 (C.T.J.). J.A.W. acknowledges support under the Georgia Tech President's

Undergraduate Research Award (PURA). The content is solely the responsibility of the authors and does not necessarily represent the official views of the National Institutes of Health.

Funding information

National Institutes of Arthritis and Musculoskeletal and Skin Diseases of the National Institutes of Health, Grant/Award Numbers: F30AR069472, R01AR062920; The Georgia Tech President's Undergraduate Research Award (PURA)

REFERENCES

Agarwal R, Johnson CT, Imhoff BR, Donlan RM, Mccarty NA, & García AJ (2018). Inhaled bacteriophage-loaded polymeric microparticles ameliorate acute lung infections. Nature Biomedical Engineering, 2 (11), 841–849.

Antoci V, Chen AF, & Parvizi J (2017). Orthopedic implant use and infection In Ducheyne P (Ed.), Comprehensive Biomaterials II (pp. 133–151). Oxford: Elsevier.

Berríos-Torres SI, Umscheid CA, Bratzler DW, Leas B, Stone EC, Kelz RR, …Schecter WP (2017). Centers for Disease Control and Prevention guideline for the prevention of surgical site infection, 2017. JAMA Surgery, 152(8), 784. [PubMed: 28467526]

Brady RA, Leid JG, Calhoun JH, Costerton JW, & Shirtliff ME (2008). Osteomyelitis and the role of biofilms in chronic infection. FEMS Immunology and Medical Microbiology, 52(1), 13–22. [PubMed: 18081847]

Brouqui P, Rousseau MC, Stein A, Drancourt M, & Raoult D (1995). Treatment of Pseudomonas aeruginosa-infected orthopedic prostheses with ceftazidime-ciprofloxacin antibiotic combination. Antimicrobial Agents and Chemotherapy, 39(11), 2423–2425. [PubMed: 8585720]

Bruttin A, & Brussow H (2005). Human volunteers receiving Escherichia coliphage T4 orally: A safety test of phage therapy. Antimicrobial Agents and Chemotherapy, 49(7), 2874–2878. [PubMed: 15980363]

Bryers JD (2008). Medical biofilms. Biotechnology and Bioengineering, 100(1), 1–18. [PubMed: 18366134]

Campoccia D, Montanaro L, & Arciola CR (2006). The significance of infection related to orthopedic devices and issues of antibiotic resistance. Biomaterials, 27(11), 2331–2339. [PubMed: 16364434]

Caplin JD, & García AJ (2019). Implantable antimicrobial biomaterials for local drug delivery in bone infection models. Acta Biomaterialia, 93,2–11. [PubMed: 30654212]

Ceri H, Olson ME, Stremick C, Read RR, Morck D, & Buret A (1999). The Calgary biofilm device: new technology for rapid determination of antibiotic susceptibilities of bacterial biofilms. Journal of Clinical Microbiology, 37(6), 1771–1776. [PubMed: 10325322]

Chanishvili N, Chanishvili T, Tediashvili M, & Barrow P (2001). Phages and their application against drug-resistant bacteria. Journal of Chemical Technology & Biotechnology, 76(7), 689–699.

Chibani-Chennoufi S, Sidoti J, Bruttin A, Kutter E, Sarker S, & Brussow H (2004). In vitro and in vivo Bacteriolytic activities of Escherichia coli Phages: Implications for phage therapy. Antimicrobial Agents and Chemotherapy, 48(7), 2558–2569. [PubMed: 15215109]

Cornelissen A, Ceyssens P, Tsyen J, Praet HV, Noben J, Shaburova OV, … Lavigne R (2011). The T7-related Pseudomonas putida phage φ15 displays Virion-associated biofilm degradation properties. PLoS One, 6(4), e18597.

Curtin JJ, & Donlan RM (2006). Using bacteriophages to reduce formation of catheter-associated biofilms by Staphylococcus epidermidis. Antimicrobial Agents and Chemotherapy, 50(4), 1268–1275. [PubMed: 16569839]

Dedrick RM, Guerrero-Bustamante CA, Garlena RA, Russell DA, Ford K, Harris K, … Spencer H (2019). Engineered bacteriophages for treatment of a patient with a disseminated drug-resistant Mycobacterium abscessus. Nature Medicine, 25(5), 730–733.

Erol S, Altoparlak U, Akcay MN, Celebi F, & Parlak M (2004). Changes of microbial flora and wound colonization in burned patients. Burns, 30(4), 357–361. [PubMed: 15145194]

Escapa IF, Cerro CD, García JL, & Prieto MA (2012). The role of GlpR repressor in Pseudomonas putida KT2440 growth and PHA production from glycerol. Environmental Microbiology, 15(1), 93–110. [PubMed: 22646161]

Flemming H, & Wingender J (2010). The biofilm matrix. Nature Reviews Microbiology, 8(9), 623–633. [PubMed: 20676145]

Fu W, Forster T, Mayer O, Curtin JJ, Lehman SM, & Donlan RM (2009). Bacteriophage cocktail for the prevention of biofilm formation by Pseudomonas aeruginosa on catheters in an in vitro model system. Antimicrobial Agents and Chemotherapy, 54(1), 397–404. [PubMed: 19822702]

García JR, Clark AY, & García AJ (2016). Integrin-specific hydrogels functionalized with VEGF for vascularization and bone regeneration of critical-size bone defects. Journal of Biomedical Materials Research Part A, 104(4), 889–900. [PubMed: 26662727]

Gbejuade HO, Lovering AM, & Webb JC (2014). The role of microbial biofilms in prosthetic joint infections. Acta Orthopaedica, 86(2), 147–158. [PubMed: 25238433]

Hagihara M, Crandon JL, & Nicolau DP (2012). The efficacy and safety of antibiotic combination therapy for infections caused by gram-positive and gram-negative organisms. Expert Opinion on Drug Safety, 11(2), 221–233. [PubMed: 22074343]

Harper D, Parracho H, Walker J, Sharp R, Hughes G, Werthén M, … Morales S (2014). Bacteriophages and biofilms. Antibiotics, 3(3), 270–284.

Hidron AI, Edwards JR, Patel J, Horan TC, Sievert DM, Pollock DA, & Fridkin SK (2008). Antimicrobial-resistant pathogens associated with healthcare-associated infections: Annual summary of data reported to the National Healthcare Safety Network at the Centers for Disease Control and Prevention, 2006–2007. Infection Control and Hospital Epidemiology, 29(11), 996–1011. [PubMed: 18947320]

Hirsch EB, & Tam VH (2010). Impact of multidrug-resistant Pseudomonas aeruginosa infection on patient outcomes. Expert Review of Pharmacoeconomics & Outcomes Research, 10(4), 441–451. [PubMed: 20715920]

Inzana JA, Schwarz EM, Kates SL, & Awad HA (2016). Biomaterials approaches to treating implant-associated osteomyelitis. Biomaterials, 81, 58–71. [PubMed: 26724454]

Jennes S, Merabishvili M, Soentjens P, Pang KW, Rose T, Keersebilck E, … Pirnay JP (2017). Use of bacteriophages in the treatment of colistin-only-sensitive Pseudomonas aeruginosa septicaemia in a patient with acute kidney injury—A case report. Critical Care, 21(1), 129. [PubMed: 28583189]

Johnson CT, Wroe JA, Agarwal R, Martin KE, Guldberg RE, Donlan RM, …García AJ (2018). Hydrogel delivery of lysostaphin eliminates orthopedic implant infection by Staphylococcus aureus and supports fracture healing. Proceedings of the National Academy of Sciences, 115(22), E4960–E4969.

Johnson CT, Sok MCP, Martin KE, Kalelkar PP, Caplin JD, Botchwey EA, & García AJ (2019). Lysostaphin and BMP-2 co-delivery reduces S. aureus infection and regenerates critical-sized segmental bone defects. Science Advances, 5(5), eaaw1228. 10.1126/sciadv.aaw1228

Kaur S, Harjai K, & Chhibber S (2014). Bacteriophage mediated killing of Staphylococcus aureus in vitro on orthopaedic K wires in presence of linezolid prevents implant colonization. PLoS One, 9(3), e90411.

Kaur S, Harjai K, & Chhibber S (2016). In vivo assessment of phage and linezolid based implant coatings for treatment of methicillin Resistant S. aureus (MRSA) mediated orthopaedic device related infections. PLoS One, 11(6), e0157626.

Kievit TR (2009). Quorum sensing in Pseudomonas aeruginosa biofilms. Environmental Microbiology, 11(2), 279–288. [PubMed: 19196266]

Kishor C, Mishra R, Saraf S, Kumar M, Srivastav A, & Nath G (2016). Phage therapy of staphylococcal chronic osteomyelitis in experimental animal model. Indian Journal of Medical Research, 143(1), 87. [PubMed: 26997019]

Knapp CW, Dolfing J, Ehlert PA, & Graham DW (2010). Evidence of increasing antibiotic resistance gene abundances in archived soils since 1940. Environmental Science & Technology, 44(2), 580–587. [PubMed: 20025282]

Kurtz S (2007). Projections of primary and revision hip and knee Arthroplasty in the United States from 2005 to 2030. The Journal of Bone and Joint Surgery, 89(4), 780. [PubMed: 17403800]

Lehman SM, & Donlan RM (2014). Bacteriophage-mediated control of a two-species biofilm formed by microorganisms causing catheter-associated urinary tract infections in an in vitro urinary catheter model. Antimicrobial Agents and Chemotherapy, 59(2), 1127–1137. [PubMed: 25487795]

Lenski RE, & Levin BR (1985). Constraints on the coevolution of Bacteria and virulent phage: A model, some experiments, and predictions for natural communities. The American Naturalist, 125(4), 585–602.

Lister PD, Wolter DJ, & Hanson ND (2009). Antibacterial-resistant Pseudomonas aeruginosa: Clinical impact and complex regulation of chromosomally encoded resistance mechanisms. Clinical Microbiology Reviews, 22(4), 582–610. [PubMed: 19822890]

McConoughey SJ, Howlin R, Granger JF, Manring MM, Calhoun JH, Shirtliff M, … Stoodley P (2014). Biofilms in periprosthetic orthopedic infections. Future Microbiology, 9(8), 987–1007. [PubMed: 25302955]

Merabishvili M, Pirnay J, Verbeken G, Chanishvili N, Tediashvili M, Lashkhi N, … Vaneechoutte M (2009). Quality-controlled small-scale production of a well-defined bacteriophage cocktail for use in human clinical trials. PLoS One, 4(3), e4944.

Meurice E, Rguiti E, Brutel A, Hornez J-C, Leriche A, Descamps M, & Bouchart F (2012). New antibacterial microporous CaP materials loaded with phages for prophylactic treatment in bone surgery. Journal of Materials Science: Materials in Medicine, 23(10), 2445–2452. [PubMed: 22802104]

Mizoguchi K, Morita M, Fischer CR, Yoichi M, Tanji Y, & Unno H (2003). Coevolution of bacteriophage PP01 and Escherichia coli O157: H7 in continuous culture. Applied and Environmental Microbiology, 69(1), 170–176. [PubMed: 12513992]

Moriarty TF, Kuehl R, Coenye T, Metsemakers W, Morgenstern M, Schwarz EM, … Richards RG (2016). Orthopaedic device-related infection: Current and future interventions for improved prevention and treatment. EFORT Open Reviews, 1(4), 89–99. [PubMed: 28461934]

Nir-Paz R, Gelman D, Khouri A, Sisson BM, Fackler J, Alkalay-Oren S, … Hazan R (2019). Successful treatment of antibiotic-resistant, poly-microbial bone infection with bacteriophages and antibiotics combination. Clinical Infectious Diseases, ciz222 [Epub ahead of print].

Paramythiotou E, Lucet J, Timsit J, Vanjak D, Paugam-Burtz C, Trouillet J, … Andremont A (2004). Acquisition of multidrug-resistant Pseudomonas aeruginosa in patients in intensive care units: Role of antibiotics with Antipseudomonal activity. Clinical Infectious Diseases, 38(5), 670–677. [PubMed: 14986251]

Patterson J, & Hubbell J (2010). Enhanced proteolytic degradation of molecularly engineered PEG hydrogels in response to MMP-1 and MM. Biomaterials, 31(30), 7836–7845. [PubMed: 20667588]

Phee A, Bondy-Denomy J, Kishen A, Basrani B, Azarpazhooh A, & Maxwell K (2013). Efficacy of bacteriophage treatment on Pseudomonas aeruginosa biofilms. Journal of Endodontics, 39(3), 364–369. [PubMed: 23402508]

Phelps EA, Enemchukwu NO, Fiore VF, Sy JC, Murthy N, Sulchek TA, …García AJ (2011). Maleimide cross-linked bioactive PEG hydrogel exhibits improved reaction kinetics and cross-linking for cell encapsulation and in situ delivery. Advanced Materials, 24(1), 64–70. [PubMed: 22174081]

Rhoads D , Wolcott R , Kuskowski M, Wolcott B , Ward L& Sulakvelidze A (2009). Bacteriophage therapy of venous leg ulcers in humans: Results of a phase I safety trial. Journal of Wound Care, 18(6), 237–243. [PubMed: 19661847]

Rodesney CA, Roman B, Dhamani N, Cooley BJ, Touhami A, & Gordon VD (2017). Mechanosensing of shear by Pseudomonas aeruginosa leads to increased levels of the cyclic-di-GMP signal initiating biofilm development. Proceedings of the National Academy of Sciences, 114(23), 5906–5911.

Sarker SA, Mccallin S, Barretto C, Berger B, Pittet A, Sultana S, … Brüssow H (2012). Oral T4-like phage cocktail application to healthy adult volunteers from Bangladesh. Virology, 434(2), 222–232. [PubMed: 23102968]

Schindler CA, & Schuhardt VT (1964). Lysostaphin: A new Bacteriolytic agent for the Staphylococcus. Proceedings of the National Academy of Sciences of the United States of America, 51(3), 414–421. [PubMed: 14171453]

Schooley RT, Biswas B, Gill JJ, Hernandez-Morales A, Lancaster J, Lessor L, … Hamilton T (2017). Development and use of personalized bacteriophage-based therapeutic cocktails to treat a patient with a disseminated resistant Acinetobacter baumannii infection. Antimicrobial Agents and Chemotherapy, 61(10), e00954–e00917.

Shekaran A, García JR, Clark AY, Kavanaugh TE, Lin AS, Guldberg RE, & García AJ (2014). Bone regeneration using an alpha 2 beta 1 integrin-specific hydrogel as a BMP-2 delivery vehicle. Biomaterials, 35(21), 5453–5461. [PubMed: 24726536]

Silva-Rocha R, Martínez-García E, Calles B, Chavarría M, Arce-Rodríguez A, de Las Heras A, … de Lorenzo V (2012). The standard European vector architecture (SEVA): A coherent platform for the analysis and deployment of complex prokaryotic phenotypes. Nucleic Acids Research, 41, D666–D675. [PubMed: 23180763]

Smith HW, & Huggins MB (1982). Successful treatment of experimental Escherichia coliinfections in mice using phage: Its general superiority over antibiotics. Microbiology, 128(2), 307–318.

Stewart PS, & Costerton JW (2001). Antibiotic resistance of bacteria in biofilms. The Lancet, 358(9276), 135–138.

Sweere JM, Belleghem JDV, Ishak H, Bach MS, Popescu M, Sunkari V, … Bollyky PL (2019). Bacteriophage trigger antiviral immunity and prevent clearance of bacterial infection. Science, 363 (6434), eaat9691.

Thakore RV, Greenberg SE, Shi H, Foxx AM, Francois EL, Prablek MA, … Sethi MK (2015). Surgical site infection in orthopedic trauma: A case-control study evaluating risk factors and cost. Journal of Clinical Orthopaedics and Trauma, 6(4), 220–226. [PubMed: 26566333]

Tice AD (2003). Risk factors and treatment outcomes in osteomyelitis. Journal of Antimicrobial Chemotherapy, 51(5), 1261–1268. [PubMed: 12668581]

Trampuz A, & Zimmerli W (2006). Diagnosis and treatment of infections associated with fracture-fixation devices. Injury, 37(2), S59–S66.

Udou T (2004). Dissemination of nosocomial multiple-aminoglycoside-resistant Staphylococcus aureus caused by horizontal transfer of the resistance determinant (aacA/aphD) and clonal spread of resistant strains. American Journal of Infection Control, 32(4), 215–19. [PubMed: 15175616]

Webb JC, & Spencer RF (2007). The role of polymethylmethacrylate bone cement in modern orthopaedic surgery. The Journal of Bone and Joint Surgery, 89-B(7), 851–857.

Wittebole X, Roock SD, & Opal SM (2013). A historical overview of bacteriophage therapy as an alternative to antibiotics for the treatment of bacterial pathogens. Virulence, 5(1), 226–235. [PubMed: 23973944]

Wright A, Hawkins C, Änggård E, & Harper D (2009). A controlled clinical trial of a therapeutic bacteriophage preparation in chronic otitis due to antibiotic-resistant Pseudomonas aeruginosa; a preliminary report of efficacy. Clinical Otolaryngology, 34(4), 349–357. [PubMed: 19673983]

Yilmaz C, Colak M, Yilmaz BC, Ersoz G, Kutateladze M, & Gozlugol M (2013). Bacteriophage therapy in implant-related infections. The Journal of Bone and Joint Surgery-American Volume, 95(2), 117–125. [PubMed: 23324958]

Yokoe DS, Avery TR, Platt R, & Huang SS (2013). Reporting surgical site infections following Total hip and knee Arthroplasty: Impact of limiting surveillance to the operative hospital. Clinical Infectious Diseases, 57(9), 1282–1288. [PubMed: 23912846]

Zimmerli W, Lew PD, & Waldvogel FA (1984). Pathogenesis of foreign body infection. Evidence for a local granulocyte defect. Journal of Clinical Investigation, 73(4), 1191–1200. [PubMed: 6323536]

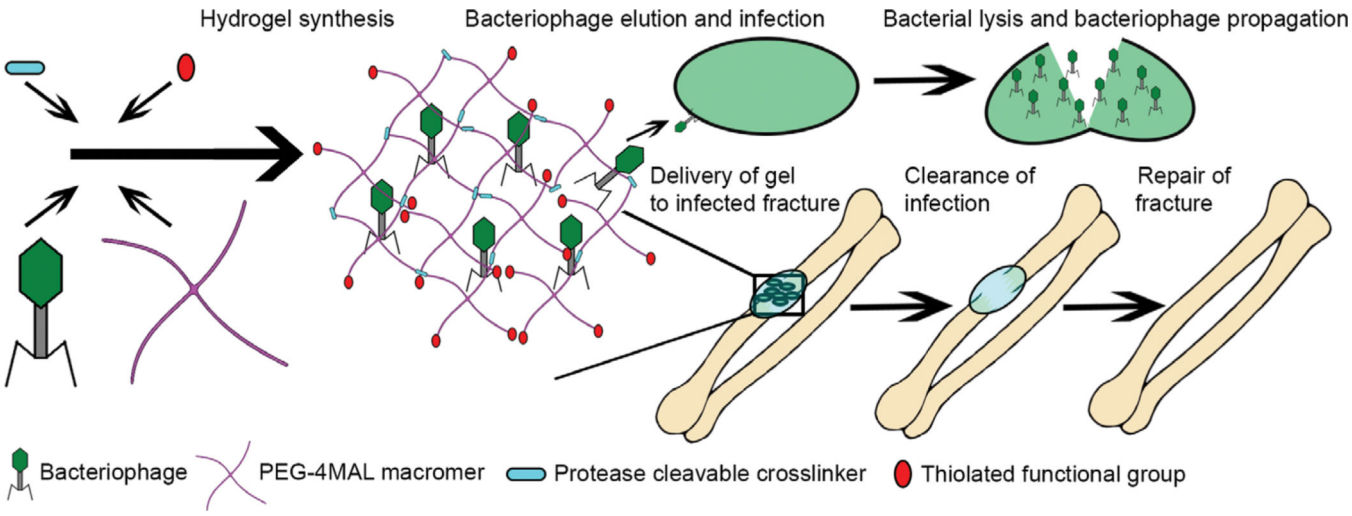

FIGURE 1.

Schematic of bacteriophage-delivering hydrogel synthesis. Thiolated crosslinker and functional components are mixed with the PEG-4MAL macromer and bacteriophage, polymerizing into a hydrogel previously developed for osseoregenerative applications, and which then releases bacteriophage to clear infection as it degrades

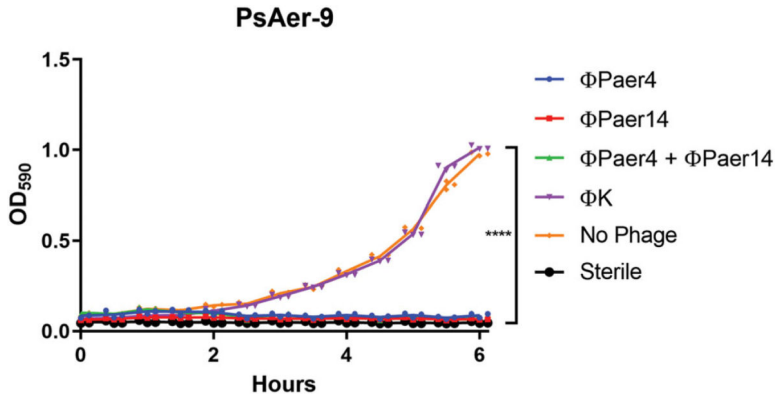

FIGURE 2.

PsAer-9 is selectively infected by *P. aeruginosa* bacteriophage. Optical density curves of liquid PsAer-9 cultures over 6 hr after treatment with *P. aeruginosa* bacteriophage (ΦPaer4, ΦPaer14) or *S. aureus* bacteriophage (ΦK). Two-way ANOVA used to compare all test groups followed by Tukey's test. Mean ± SD, $n = 3$ per group, ****$p < 0.0001$

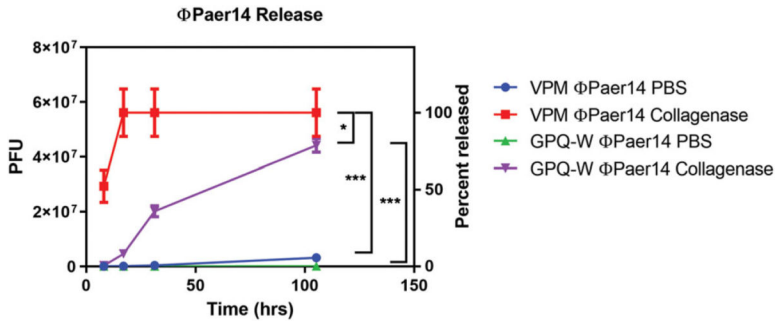

FIGURE 3.

Release of bacteriophage ΦPaer14 from two hydrogel formulations in the presence and absence of collagenase. Two-way ANOVA with Tukey's post hoc comparison test between all groups. 25 μl gels containing 1 mM RGD, 5.6×10^7 PFU of ΦPaer14, crosslinked as specified. Mean ± SD, $n = 3–4$ per group, *$p < 0.05$, ***$p < 0.001$

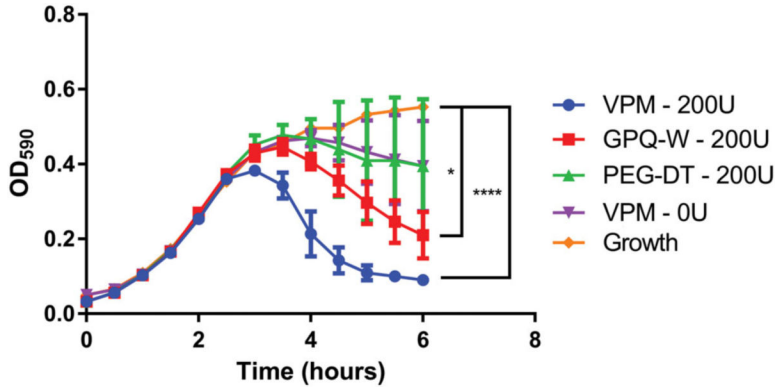

FIGURE 4.

Growth of PsAer-9 as measured by optical density of liquid cultures in the presence of bacteriophage-encapsulating hydrogels. 25 μl gels containing 1 mM RGD, 8.0×10^6 PFU each of ΦPaer4, ΦPaer14, ΦPaer22, and ΦW2005A, and 5.6×10^7 CFU/ml of PsAer-9. Crosslinked as specified. Two-way ANOVA with Tukey's post hoc comparison test comparing each group to standard growth curve. Mean ± SD, $n = 5$ per group, $^*p < 0.05$, $^{****}p < 0.0001$. CFU, Colony-forming unit; PFU, plaque forming unit

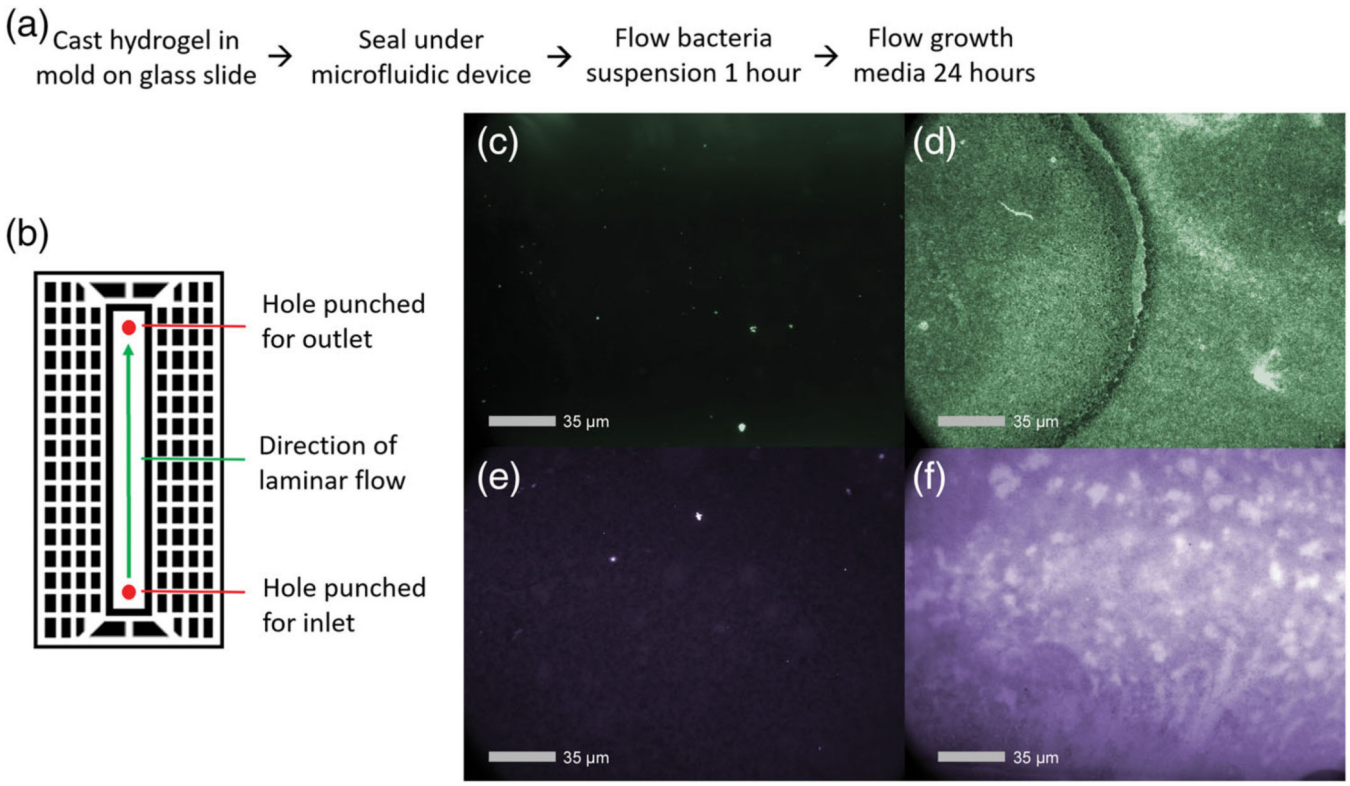

FIGURE 5.

Assembly and demonstration of microfluidic device for in vitro biofilm growth. (a) General procedure for device assembly. (b) Schematic of microfluidic device. (c,d) images of live bacteria and (e,f) biofilm matrix proteins under (c,e) static and (d,f) laminar flow conditions after 24 hr. 25 μl gels containing 1 mM RGD, 1.0×10^7 PFU of ΦPaer14 per gel, crosslinked with VPM

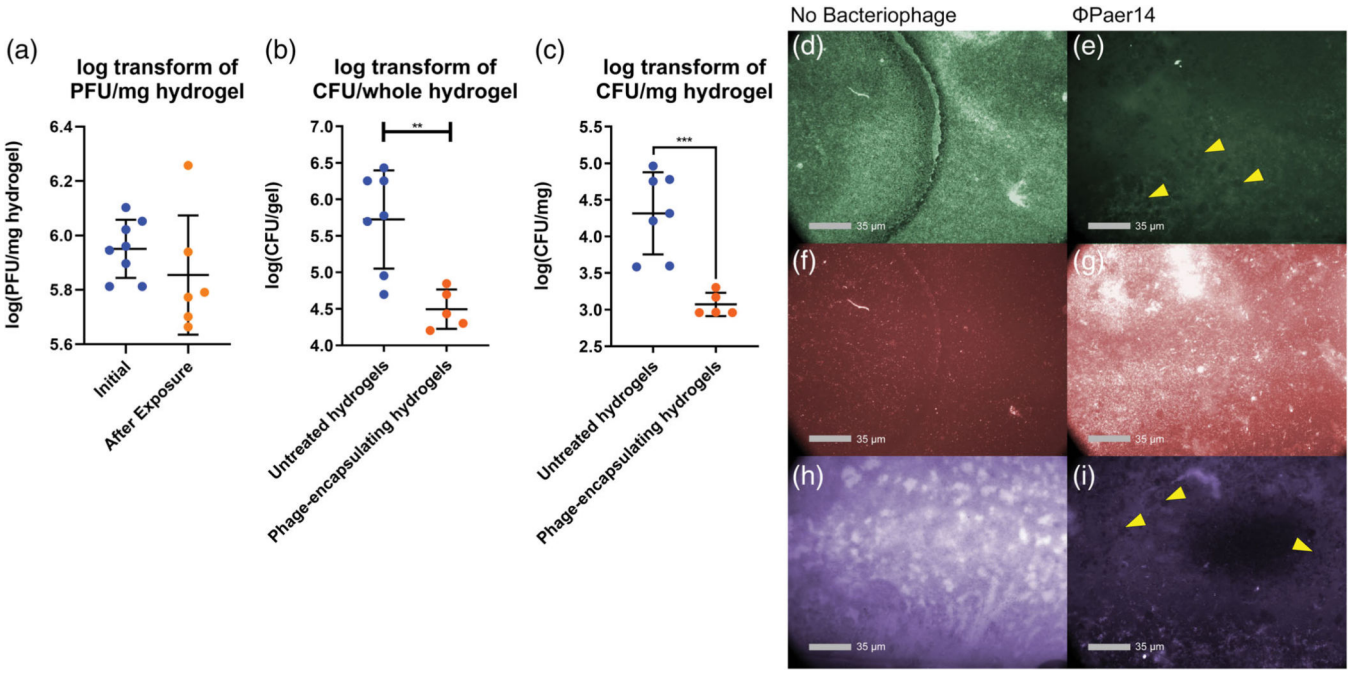

FIGURE 6.

Characterization of biofilm growth and bacteriophage survival in ΦPaer14-encapsulating hydrogels in vitro. Bacterial and bacteriophage concentration reported as log transform of CFU/PFU per mg of hydrogel (a,b) or per whole hydrogel (c). (a) Viable ΦPaer14 encapsulated in hydrogels before and after 24-hr biofilm generation protocol. (b,c) concentration of live PsAer-9 recovered from biofilms grown on untreated and ΦPaer14-encapsulating hydrogels. (d-i) fluorescent staining of live bacteria (d,e), dead bacteria (f,g), and biofilm-associated proteins (h,i) after 24-hr biofilm generation protocol on untreated and bacteriophage-encapsulating hydrogels. 25 μl gels containing 1 mM RGD, 1.0×10^7 PFU of ΦPaer14 per gel, crosslinked with VPM. Two-tailed *t* test. Mean ± SEM, $n = 5–8$ per group, $*p < 0.05$ $**p < 0.001$, $***p < 0.001$, $****p < 0.0001$

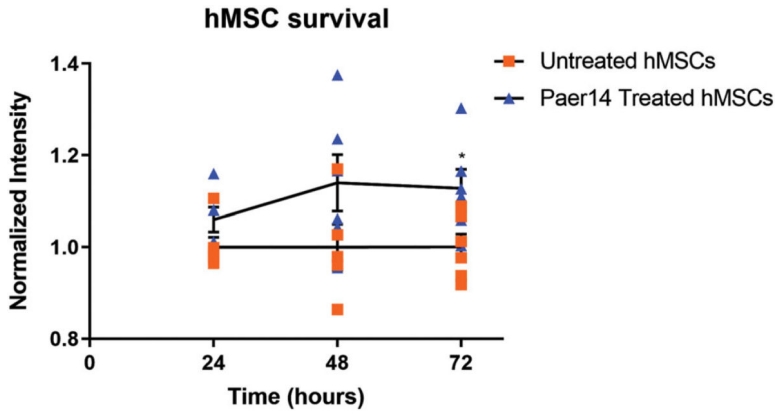

FIGURE 7.

Tolerance of bacteriophage in vitro. Metabolic activity of hMSC populations exposed to ΦPaer14 for 24,48, and 72 hr, normalized to the activity of populations grown in the absence of ΦPaer14 for the same period of time. Two-way ANOVA with Tukey's post hoc comparison test comparing each ΦPaer14 group to the untreated group at the same time point. Mean ± *SD*, $n = 6$ per group, $*p < 0.05$

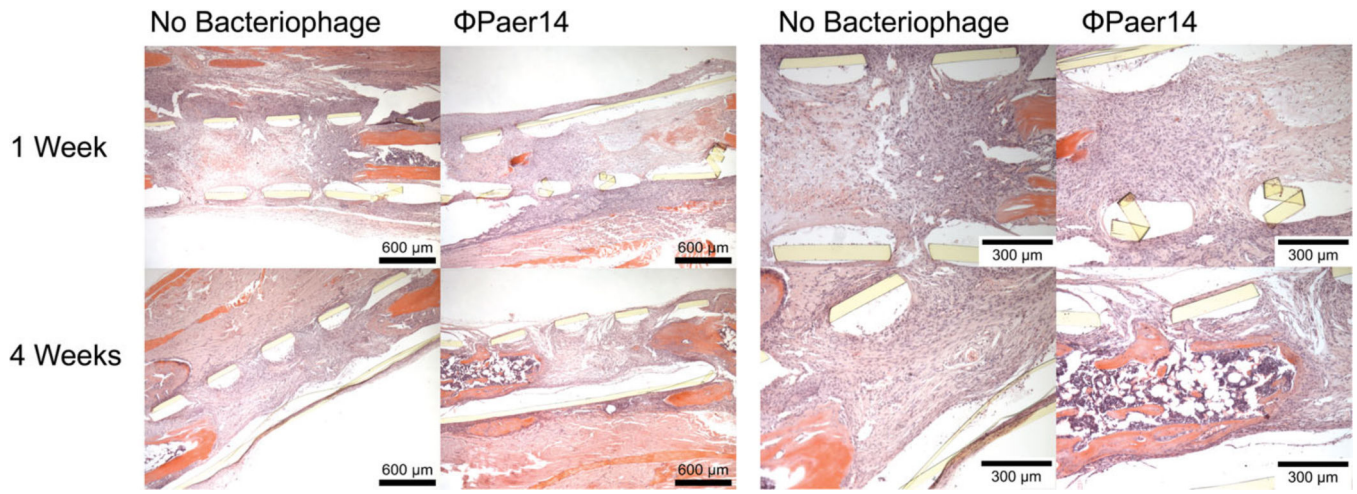

FIGURE 8.

Histological sections of implant site 7 and 28 days after delivery of untreated or bacteriophage-encapsulating hydrogels to radial defect in mice. 5 μl gels containing 1 mM GFOGER, 30 ng BMP-2, 5 × 108 PFU/ml ΦPaer14, crosslinked with VPM

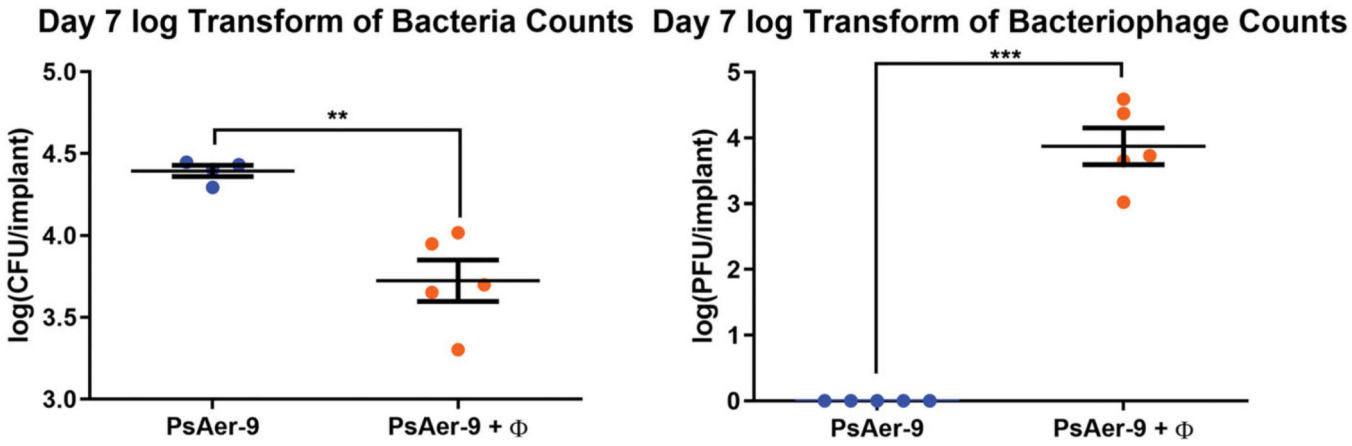

FIGURE 9.

In vivo characterization of the efficacy and tolerance of bacteriophage-encapsulating hydrogels in a murine radial segmental defect model. (a) Log transform of live PsAer-9 recovered from in an infected radial defect model treated standard and bacteriophage-encapsulating hydrogels. (b) Log transform of live bacteriophage recovered from in an infected radial defect model treated with standard and bacteriophage-encapsulating hydrogels. 3 μl gels containing 1 mM GFOGER, 30 ng BMP-2,1.2e8 PFU/ml each of ΦPaer4, ΦPaer14, ΦPaer22, and ΦW2005A, and 3.0×10^4 CFU PsAer-9, crosslinked with VPM. Two-tailed *t* test. Mean ± SEM, $n = 5$ per group, $^{**}p < 0.01$, $^{***}p < 0.001$